



The ubiquitin ligase FBXW7 targets the centriolar assembly protein HsSAS-6 for degradation and thereby regulates centriole duplication

Received for publication, December 6, 2019, and in revised form, February 19, 2020. Published, Papers in Press, February 21, 2020, DOI 10.1074/jbc.AC119.012178

Binshad Badarudeen[‡], Ria Gupta[‡], Sreeja V. Nair[‡], Aneesh Chandrasekharan[§], and Tapas K. Manna^{‡1}

From the [‡]School of Biology, Indian Institute of Science Education and Research, Thiruvananthapuram, Vithura, Thiruvananthapuram 695551, Kerala, India and the [§]Rajiv Gandhi Centre for Biotechnology, Thiruvananthapuram 695014, Kerala, India

Edited by Patrick Sung

Formation of a single new centriole from a pre-existing centriole is strictly controlled to maintain correct centrosome number and spindle polarity in cells. However, the mechanisms that govern this process are incompletely understood. Here, using several human cell lines, immunofluorescence and structured illumination microscopy methods, and ubiquitination assays, we show that the E3 ubiquitin ligase F-box and WD repeat domain-containing 7 (FBXW7), a subunit of the SCF ubiquitin ligase, down-regulates spindle assembly 6 homolog (HsSAS-6), a key protein required for procentriole cartwheel assembly, and thereby regulates centriole duplication. We found that FBXW7 abrogation stabilizes HsSAS-6 and increases its recruitment to the mother centriole at multiple sites, leading to supernumerary centrioles. Ultrastructural analyses revealed that FBXW7 is broadly localized on the mother centriole and that its presence is reduced at the site where the HsSAS-6-containing procentriole is formed. This observation suggested that FBXW7 restricts procentriole assembly to a specific site to generate a single new centriole. In contrast, during HsSAS-6 overexpression, FBXW7 strongly associated with HsSAS-6 at the centriole. We also found that SCF^{FBXW7} interacts with HsSAS-6 and targets it for ubiquitin-mediated degradation. Further, we identified putative phosphodegron sites in HsSAS-6, whose substitutions rendered it insensitive to FBXW7-mediated degradation and control of centriole number. In summary, SCF^{FBXW7} targets HsSAS-6 for degradation and thereby controls centriole biogenesis by restraining HsSAS-6 recruitment to the mother centriole, a molecular mechanism that controls supernumerary centrioles/centrosomes and the maintenance of bipolar spindles.

Maintenance of correct centrosome/centriole number in cells is crucial for genetic stability and tissue homeostasis (1, 2). In the proliferating cells, each centriole of an interphase centrosome duplicates strictly once during the cell cycle to gener-

ate two centrosomes that direct bipolar spindle assembly, a prerequisite for faithful segregation of chromosomes (3, 4). Failure of centriole duplication leads to mitotic cells with monopolar spindles, whereas its overduplication results in supernumerary centrosomes and multipolar spindles (5–7). During G₁/S entry of the cell cycle, each mother centriole starts assembling only a single new centriole, called the procentriole, at a specific site toward its proximal end. The molecular processes that control formation of only one procentriole per mother centriole remain poorly understood.

The procentriole is assembled through an evolutionarily conserved pathway involving key proteins that include Plk4/Sak/ZYG-1, Cep192/DSPd-2/SPD-2, HsSAS-6/DSas-6/Sas-6, STIL/Ana2/SAS-5, and CPAP/DSas-4/SAS-4 (8–13). Studies in *Drosophila* and human cells have also identified another factor, Asterless/Cep152, that is required at the very early stage of procentriole formation (14–17). A critical step of procentriole formation is the assembly of a cartwheel-like template on the mother centriole, onto which the triplet microtubules are polymerized (18–21). The main component of the procentriole cartwheel is SAS-6, an evolutionarily conserved coiled-coil protein (9), whose oligomerization leads to cartwheel-like assembly of the procentriole (18, 22–27). SAS-6 recruitment and the cartwheel assembly begin at the G₁/S entry of the cell cycle, and thereafter, formation of the new centriole resumes (28–30). Depletion of SAS-6 leads to failure of daughter centriole formation, whereas its overexpression generates supernumerary centrioles (25, 28, 31).

Recent studies have implicated roles of ubiquitin-mediated protein degradation in regulating the functions of centrosome/centrioles (28, 32–35). One such key regulator is SCF^{FBXW7} with its substrate targeting subunit FBXW7, an evolutionarily conserved E3 ligase (36). FBXW7 is mutated in numerous cancers and is linked to chromosomal instability and tumorigenesis (36–38). Recently, FBXW7 abrogation has been shown to negatively regulate cilia assembly, a process that requires functional integrity of the centriole (39). Furthermore, FBXW7 expression bears a negative correlation with centriole number in cells (40). However, the molecular link of FBXW7 to centriole amplification is not clearly understood.

Here, we demonstrate that SCF^{FBXW7} targets HsSAS-6 for degradation and thereby controls centriole biogenesis by restraining HsSAS-6 recruitment to the mother centriole.

This work was supported by DST-SERB, Government of India, and by an INSPIRE fellowship from DST, Government of India (to B. B.). The authors declare that they have no conflicts of interest with the contents of this article.

This article contains supporting Experimental procedures and Figs. S1 and S2.
¹ To whom correspondence should be addressed. Tel.: 91-471-2778172; E-mail: tmanna@iisertvm.ac.in.

Ultrastructural analyses reveal direct association of FBXW7 with HsSAS-6 and its unique localization on mother centriole that ensures HsSAS-6 recruitment to a specific site to form the new centriole. Biochemical results demonstrate ubiquitin-mediated degradation of HsSAS-6 by SCF^{FBXW7}. Our data for the first time provide a molecular basis for the control of supernumerary centrioles and centrosome amplification in human cells.

Results and discussion

FBXW7 controls centriole duplication by regulating HsSAS-6 at the centrioles

We first analyzed centriole numbers both in FBXW7 knock-out (KO) FBXW7^{-/-} DLD-1 cells (38) and in HeLa cells depleted of FBXW7 by esiRNA. Formation of extra (more than four) centrioles was induced in both cases in the G₁/S synchronized condition (Fig. 1 (a and b) and Fig. S1 (a and b)). The percentage of cells with more than four centrioles was ~3-fold higher (19% versus 6%) in FBXW7 KO cells as compared with FBXW7 WT cells (Fig. 1b and Fig. S1b). We then inspected how loss of FBXW7 affects procentriole assembly proteins at the centrosome. HsSAS-6 was found to be localized specifically to each of the supernumerary centrioles in the KO or depleted cells (Fig. 1c and Fig. S1 (c and d)). Total centrosomal HsSAS-6 intensity was increased (Fig. 1d). Plk4 appeared to localize to each of those centrioles, but its overall level did not seem to increase (Fig. S1e). Co-staining of HsSAS-6 with mother centriole marker, Odf2, showed multiple HsSAS-6 foci surrounding a single Odf2-stained centriole, indicating that the extra procentrioles were generated on a single mother centriole (Fig. 1e). In concurrence with supernumerary centrioles, formation of extra centrosomes and multipolar spindles were induced (Fig. 1, f and g).

We next investigated the effect of exogenous FBXW7 expression on HsSAS-6 localization. HsSAS-6 localization at centrioles was reduced in the mCherry-FBXW7-expressed U2OS G₁/S cells (Fig. 2, a and b). For intensity quantification uniformly, cells with two centrioles were selected for the analysis. Contrastingly, expression of an F-box domain-deleted variant (Fig. S1f), mCherry-FBXW7-FboxΔ, increased centriolar HsSAS-6 level, induced HsSAS-6 localization at multiple centrioles (Fig. S2a), and also showed a multipolar mitosis phenotype (Fig. 2, a and b). Consistently, when progressed to mitosis, mCherry-FBXW7-expressed cells showed a reduced number of centrioles at the spindle poles (Fig. 2, c and d). In contrast, the mCherry-FBXW7-FboxΔ induced a multipolar phenotype with extra centrioles. γ-Tubulin, CPAP, and CEP135 were not affected (Fig. 2a and Fig. S2 (b and c)). These results indicate that FBXW7 controls centriole duplication by specifically regulating HsSAS-6 at the centrosome.

We next assessed the structural organization of FBXW7 at the centrioles. Structured illumination microscopy (SIM)²

imaging of centrin-1-eGFP stable RPE-1 cells revealed that FBXW7 localizes to both the centrioles radially by covering most of the areas, but less in the areas where HsSAS-6 is localized (Fig. 3a). Three-dimensional reconstructed images showed a clearer view of such organization (Fig. 3c). A model representing FBXW7 and HsSAS-6 localization is shown in Fig. 3b. The absence of FBXW7 at and near the procentriole sites was further confirmed by co-staining FBXW7 with centrin, a daughter centriole marker (41) (Fig. 3d). However, as the centrioles were oriented randomly, it was difficult to infer from the SIM images whether FBXW7 localizes along the whole length of the centriole or in the region at and near its proximal end. Because in normal cells, FBXW7 localization was somewhat inversely correlated with HsSAS-6, we then checked whether the two proteins could associate with each other in the HsSAS-6-over-expressed condition. We imaged FBXW7 in eGFP-HsSAS-6-overexpressed HeLa Kyoto cells under treatment of protease inhibitor MG-132. Endogenous FBXW7 strongly colocalized with eGFP-HsSAS-6 at and around the centrioles (Fig. 3e). FBXW7 localized around the eGFP-HsSAS-6-stained centrioles as multiple clusters. Overall, these findings indicate that FBXW7 directly associates with HsSAS-6 at the centriole. We also imaged HsSAS-6 localization on the mother centriole in the FBXW7 KO DLD1 cells. Unlike the FBXW7 WT cells, the knockout cells showed HsSAS-6 localization at multiple sites on and around the mother centriole (Fig. 3f), suggesting deregulation of HsSAS-6 recruitment on the mother centriole.

FBXW7 targets HsSAS-6 for degradation

We next assessed whether FBXW7 regulates HsSAS-6 stability. The level of HsSAS-6 was increased significantly in FBXW7-depleted HeLa and U2OS cells (Fig. 4, a and b) and similarly in FBXW7 knockout DLD-1 cells (Fig. 4c). A ~1.5–1.8-fold increase of HsSAS-6 level as compared with control was observed in all of these cell lines (Fig. 4c). However, FBXW7 depletion did not alter Plk4 or FBXW5 (Fig. S2d) (32). We found that HsSAS-6 stabilization was pronounced maximally at G₁/S followed by S phase (Fig. 4d). A rescue experiment by expression of exogenous FLAG-FBXW7 in the knockout cells reduced HsSAS-6 to a level comparable with that of FBXW7 WT cells (Fig. 4e). We next determined the role of the WD40 substrate-binding region (Fig. S1f). Exogenously expressed Myc-HsSAS-6 level was more stabilized in FLAG-FBXW7-WDΔ cells as compared with FLAG-FBXW7 WT (Fig. 4f). Plk4 and FBXW5 did not change under similar conditions (Fig. S2e).

FBXW7 physically interacts with HsSAS-6

We next determined whether FBXW7 interacts with HsSAS-6. Co-immunoprecipitation (co-IP) in G₁/S synchronized HeLa and HEK293T cells showed the presence of HsSAS-6 in the immunoprecipitate of endogenous and FLAG-tagged FBXW7, respectively (Fig. 4, g and h). The interaction was further confirmed by reverse co-IP of endogenous HsSAS-6 in HEK293T cells (Fig. 4i). Furthermore, FLAG pull-down of WD domain-deleted FBXW7 showed no HsSAS-6,

² The abbreviations used are: SIM, structured illumination microscopy; IP, immunoprecipitation; CPD, Cdc4 phosphodegron; KO, knockout; DAPI, 4',6-diamidino-2-phenylindole; MBP, maltose-binding protein; Ub, ubiquitin.

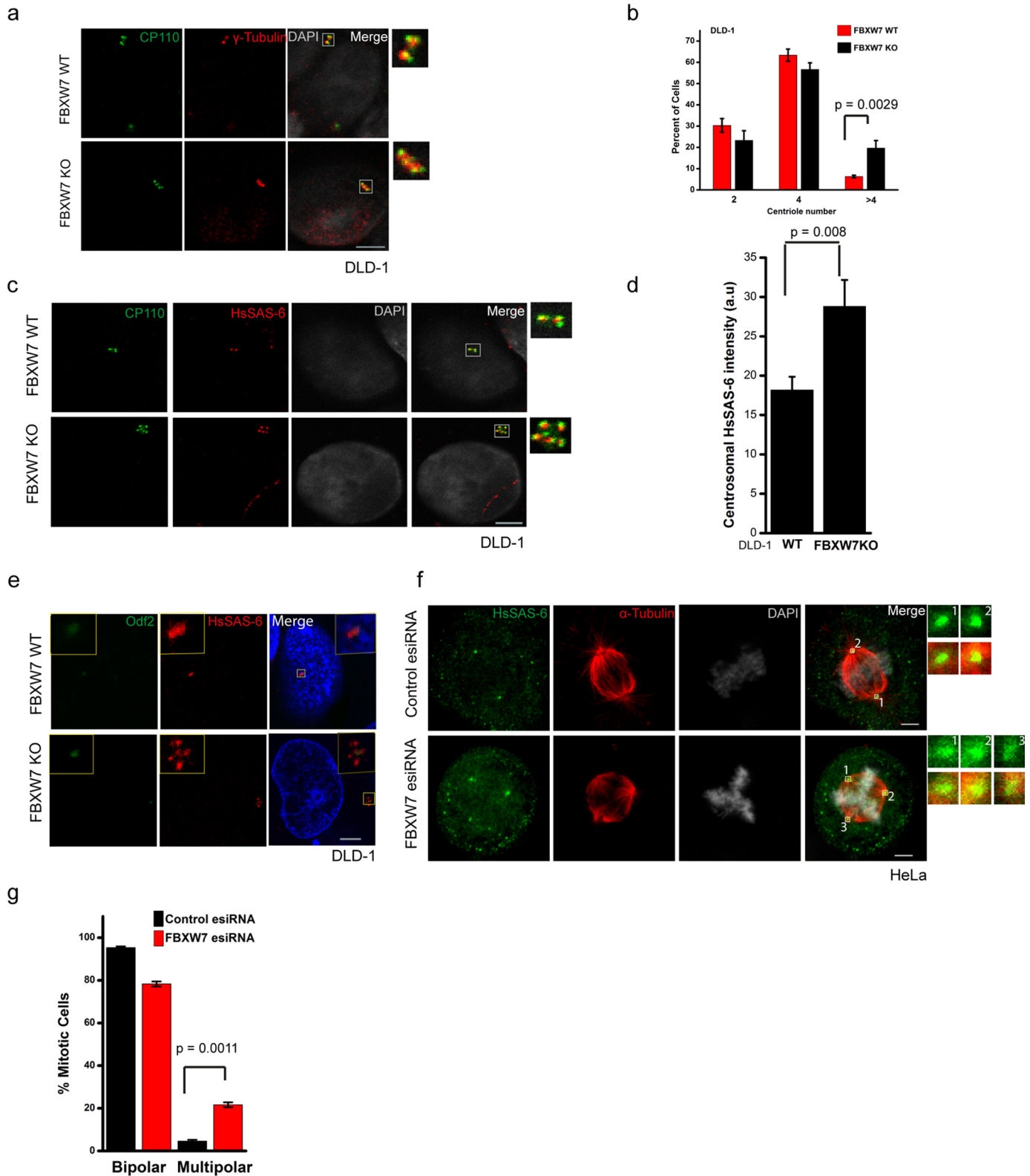


Figure 1. FBXW7 controls centriole duplication by regulating HsSAS-6 at the centrosome. *a*, representative confocal images showing supernumerary centrioles (more than four) in DLD-1 FBXW7 KO cells. *b*, plot of the percentage of cells versus centriole number in DLD-1 FBXW7 WT versus FBXW7 KO; $n \approx 80-100$ cells. *c*, G_1/S synchronized FBXW7 WT versus FBXW7 KO DLD-1 cells stained for HsSAS-6 and CP110. *d*, plot of centrosomal HsSAS-6 intensity in FBXW7 KO versus FBXW7 WT DLD-1 cells. Data are mean \pm S.D. (error bars). $n \approx 20$ cells. *e*, FBXW7 KO versus FBXW7 WT DLD-1 cells at G_1/S were stained for Odf2 and HsSAS-6. *f*, regions of individual centrosomes are indicated by boxes with numbers (1,2,3) and are displayed in enlarged forms on the right. The plot in *g* shows percentage bipolar versus multipolar cells. $n \approx 50$ mitotic cells.

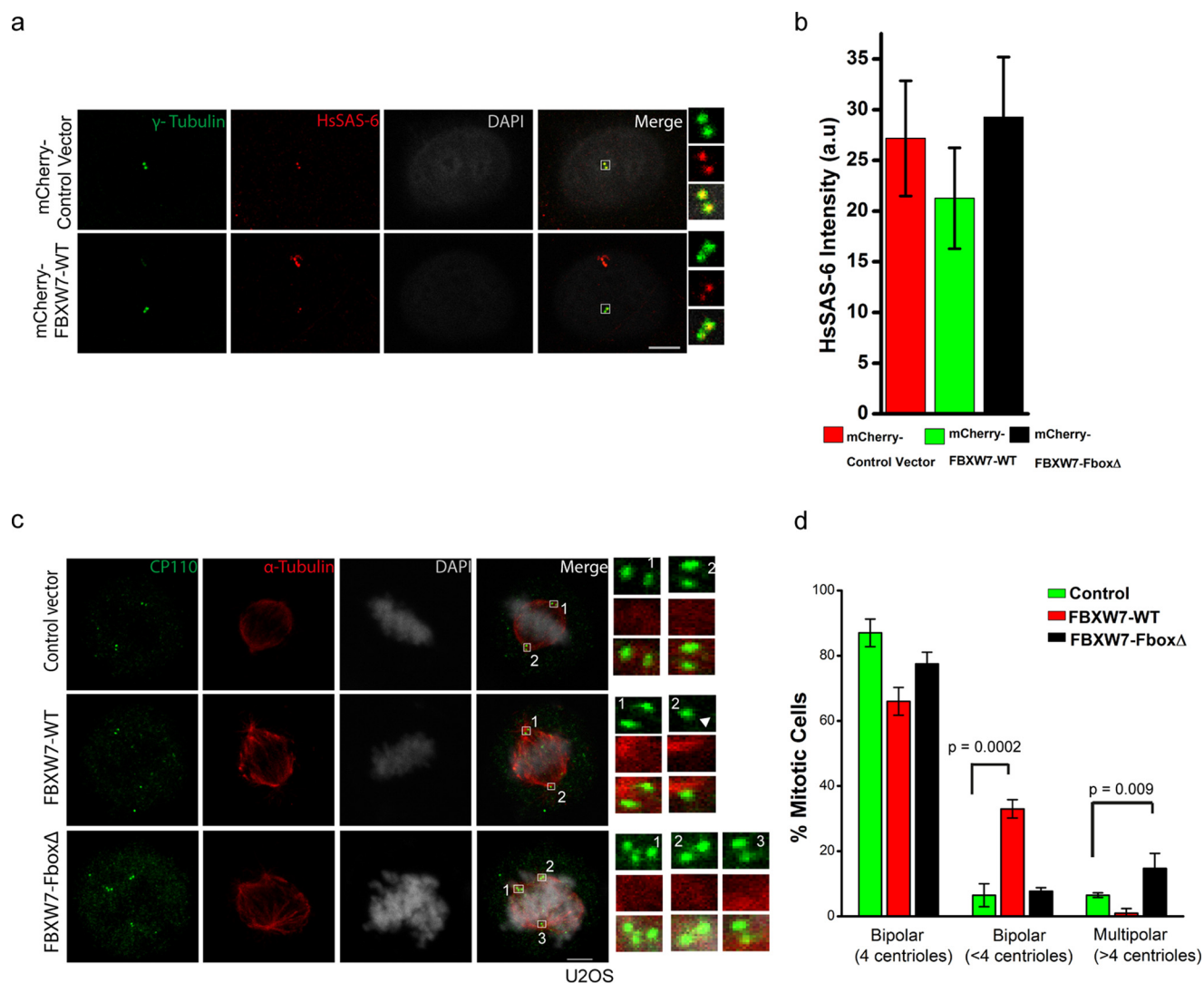


Figure 2. FBXW7 overexpression abrogates new centriole formation by diminishing HsSAS-6 at the centrosome. *a*, U2OS cells transfected with mCherry-FBXW7-WT stained for HsSAS-6 and γ -tubulin. *b*, plot of HsSAS-6 intensity at centrosome with two centrioles in FBXW7-WT versus mCherry-FBXW7-Fbox Δ condition. $n \approx 30$. *c*, mitotically synchronized U2OS cells transfected with mCherry-tagged FBXW7-WT or FBXW7-Fbox Δ were stained for CP110 and α -tubulin. Loss of centrioles at the spindle pole is indicated by an arrow. *d*, plot for percentage mitotic cells with bipolar (four centrioles), defective bipolar (less than four centrioles), and multipolar (more than four centrioles) spindles. $n \approx 50$ mitotic cells in each. Data are mean \pm S.D. (error bars) (three experiments) in all of the plots.

indicating that the WD domain is required for the interaction (Fig. 4*h*).

FBXW7 ubiquitylates HsSAS-6

We next determined whether SCF^{FBXW7} ubiquitylates HsSAS-6. We first assayed ubiquitination *in vivo* in HEK293 cells (see “Experimental procedures”). Levels of ubiquitylated proteins were substantially increased in the FLAG-FBXW7-expressed cells (Fig. 5*a*). Unlike FBXW7 WT, FLAG-FBXW7-WD Δ cells showed a very low level of ubiquitination, comparable with the control cells (Fig. 5*a*). We also checked the ubiquitination of purified recombinant MBP-tagged HsSAS-6. All of the four SCF^{FBXW7} complex components were purified from HEK293T cells by FLAG pull-down and mixed with MBP-HsSAS-6 (Fig. S2*f*) (42). MBP-HsSAS-6 was ubiquitinated in a dose-dependent manner (Fig. 5*b*). Ubiquitin-mediated destruction of substrate proteins involves formation of polyubiquitin chains through covalent conjugation through Lys

residues at 48 and 63 (43). We tested involvement of those two lysines of ubiquitin in FBXW7-mediated HsSAS-6 ubiquitination. A mixture of purified MBP-HsSAS-6 and SCF^{FBXW7} complex was incubated with either Ub WT or Ub K63R or K48R mutant in the presence of E1, E2, and ATP. HsSAS-6 ubiquitination was substantially reduced both in the Ub K63R and Ub K48R mutants as compared with Ub WT (Fig. 5*c*). Altogether, these results demonstrate that HsSAS-6 is a ubiquitylation substrate of SCF^{FBXW7}.

Putative phosphodegron sites in HsSAS-6 are involved in FBXW7 interaction

FBXW7 targets substrate proteins through the substrate consensus Cdc4 phosphodegron (CPD) motif with the sequence (S/T)PX₂(S/T/D/E/X) (where X represents any amino acid) (36, 44). In many cases, prior phosphorylation in the CPD sites is involved in substrate recognition by the ligase. Sequence analysis revealed two conserved CPD-like

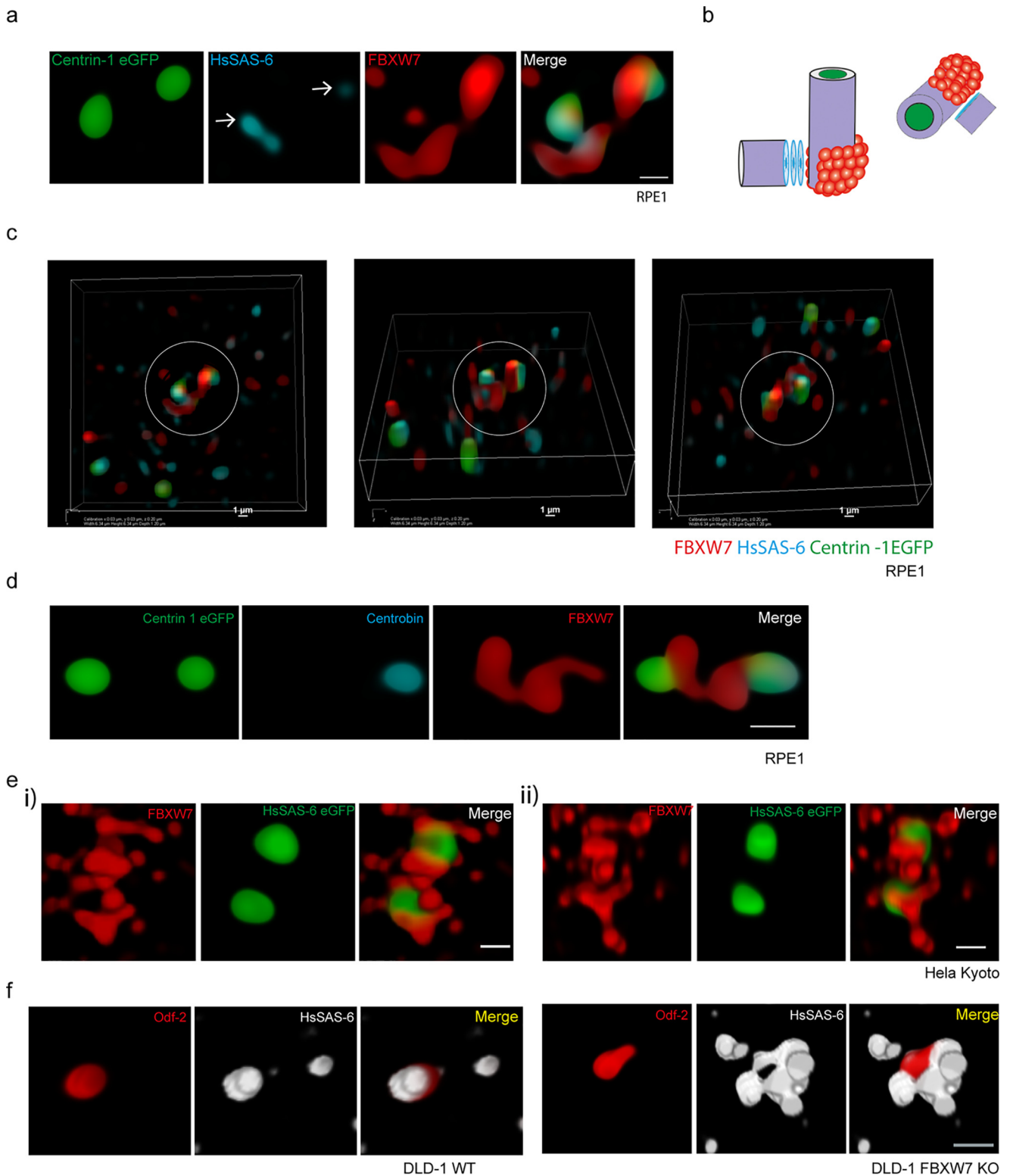


Figure 3. Organization of FBXW7 at the centrosome. *a*, reconstructed SIM images of centrioles of a G₁/S synchronized centrin-1-eGFP RPE1 cell stained for HsSAS-6 and FBXW7. HsSAS-6-stained procentrioles are shown by an *arrow*. *b*, a *cartoon* representing FBXW7 (*red*) and HsSAS-6 (*light blue*) on mother centrioles. The centriole lumen is shown by *light violet*, and centrin-1 localization in the distal lumen is shown by *green*. HsSAS-6 (*light blue*) on one centriole appeared dimmer than the other, presumably due to different orientations of the centrioles. *c*, reconstructed three-dimensional view SIM images of centrioles of RPE-1 centrin-1-eGFP cell showing FBXW7, HsSAS-6, and centrin-1 localization. Images of the same cell (as shown in *a*) in three different orientations are shown. *Scale bar*, 1 μ m. *d*, reconstructed SIM images of centrin-1-eGFP stably expressed RPE1 cell stained for centrobin and FBXW7. *e*, reconstructed SIM image in two different orientations (*i* and *ii*) of eGFP-HsSAS-6 – overexpressed HeLa Kyoto cell showing co-localization of eGFP-HsSAS-6 with endogenous FBXW7. *f*, SIM images of HsSAS-6 localization on mother centrioles in FBXW7 WT *versus* KO DLD-1 cells. Cells were stained with Odf2 and HsSAS-6 antibodies. Unless otherwise mentioned, *scale bars* of all SIM images are 500 nm.

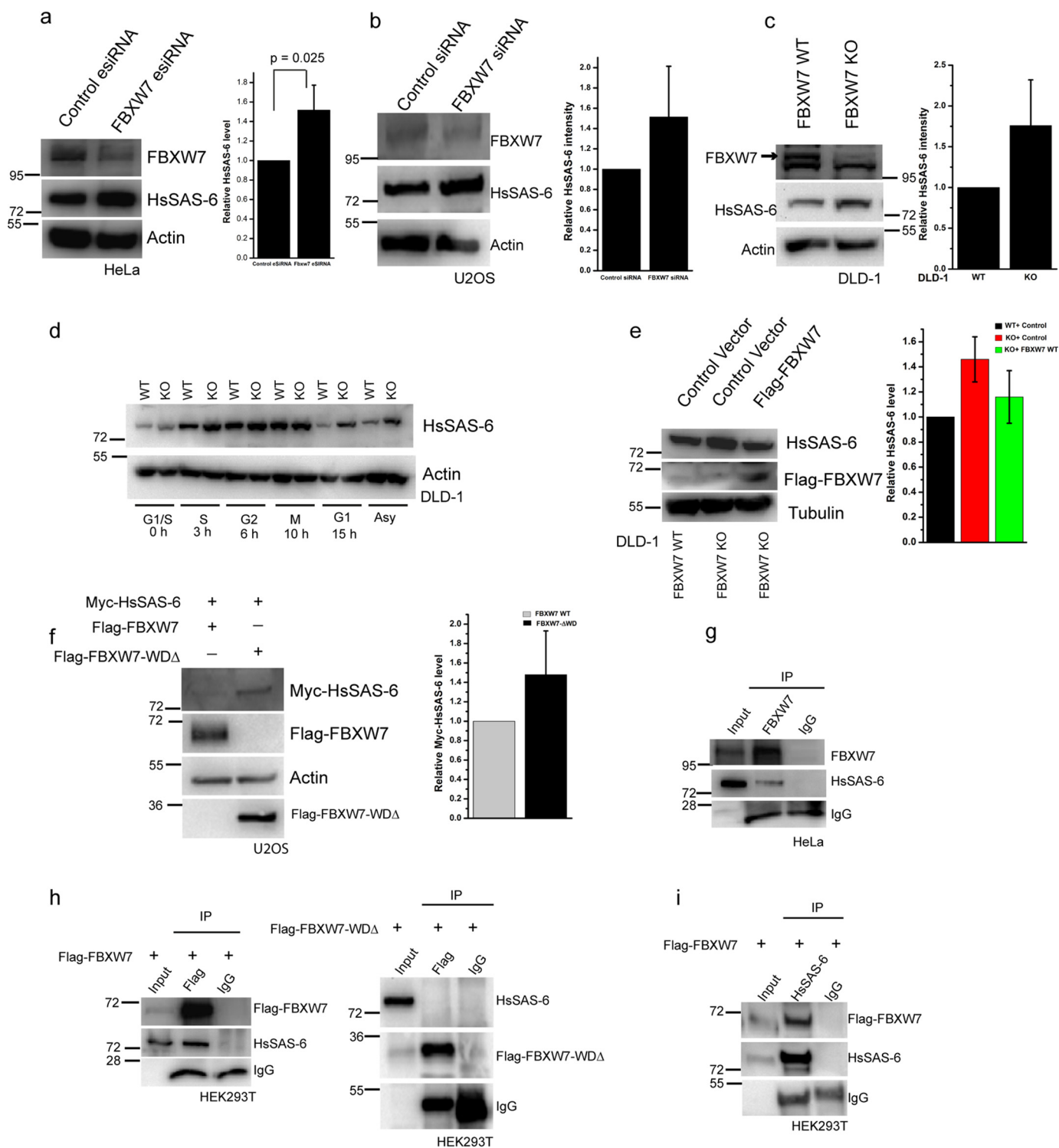
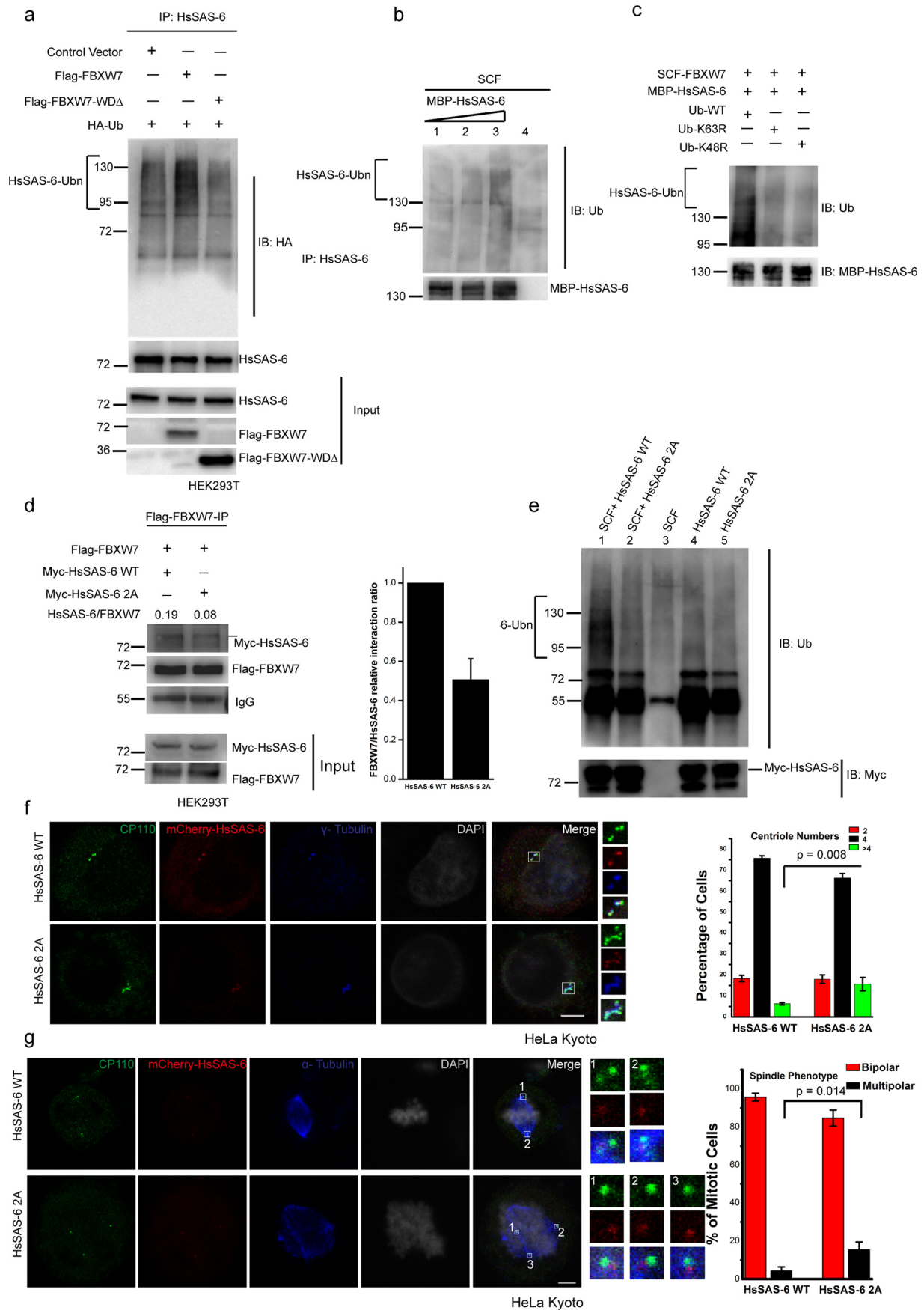


Figure 4. HsSAS-6 is a novel FBXW7 substrate. HeLa (a) or U2OS cells (b) after transfection with FBXW7 esiRNA, followed by synchronization at G₁/S, were analyzed for HsSAS-6. c, lysates of DLD-1 FBXW7 WT versus KO cells were immunoblotted for HsSAS-6. Plots of relative HsSAS-6 levels with respect to control in a–c are shown. d, representative (n = 3) HsSAS-6 levels in FBXW7 KO versus FBXW7 WT DLD-1 cells at different cell cycle stages. e, HsSAS-6 levels in the lysates of G₁/S synchronized FBXW7 WT, FBXW7 KO, and FLAG-FBXW7–expressed FBXW7 KO DLD-1 cells are co-transfected with Myc-HsSAS-6 and FLAG-FBXW7 or FLAG-FBXW7-WDΔ for 24 h followed by G₁/S synchronization were immunoblotted for Myc-HsSAS-6. g, co-IP of FBXW7 in HeLa cells shows the presence of HsSAS-6. h, lysates of HEK293T cells expressed with FLAG-FBXW7 (left) or FLAG-FBXW7-WDΔ (right) were subjected to FLAG-pulldown and probed for endogenous HsSAS-6 with FLAG-FBXW7 versus FLAG-FBXW7-WDΔ. i, co-IP of HsSAS-6 in HEK293T cells transfected with FLAG-FBXW7 (24 h) followed by G₁/S synchronization and immunoblotted for FLAG-FBXW7. In all of the plots, data are mean ± S.D. (error bars) (n = 3). Data were compared considering the control value as 1.

motifs in HsSAS-6, one at Ser-111 (SPAAI) and the other at Thr-495 (TPPAH) (Fig. S2g). We mutated these putative CPD sites Ser and Thr to alanine (2A) and checked FBXW7-

HsSAS-6 interaction and its ubiquitination. FLAG-FBXW7 interaction with Myc-HsSAS-6 was markedly reduced in the case of 2A mutant as compared with WT Myc-HsSAS-6 (Fig. 5d). An



in vitro ubiquitination assay also showed marked reduction of Myc-HsSAs-6 2A ubiquitination as compared with Myc-HsSAs-6 WT in HEK293 cells (Fig. 5*e*). We then assessed how mutation of CPD sites affects centriole duplication. Centriole amplification phenotype and multipolar spindles were more pronounced in mCherry-HsSAs-6 2A-expressed cells than the mCherry-HsSAs-6 WT cells (Fig. 5*f* and *g*) and Fig. S2*h*).

The number of centrioles/centrosomes is tightly controlled to ensure bipolar spindle assembly and genome integrity. Here, we have identified a hitherto unknown molecular mechanism that governs this process. Ultrastructural analysis of cells with overexpressed HsSAs-6 evidenced formation of multiple procentrioles on the mother centriole (28), indicating that nucleation of procentriole, in principle, can occur at multiple sites on the mother centriole. SAS-6, being the major constituent of the procentriole cartwheel, is a key player for activating the process. Our data demonstrate that FBXW7 regulates HsSAs-6 level, both at the overall cellular level and at the centrosome (Figs. 2 and 3). This is likely to be mediated by ubiquitination-mediated degradation, as our data demonstrate that HsSAs-6 is ubiquitinated by SCF^{FBXW7} (Fig. 5). Concurrent with these findings, our SIM data have supported a direct centriole-specific targeting of HsSAs-6 by FBXW7. In HsSAs-6-overexpressed cells, FBXW7 shows direct association with the centriole-localized HsSAs-6. Interestingly, the ligase appeared as multiple clusters around HsSAs-6 and centriole. Such clustering may indicate localization of FBXW7 in the form of large structures in the centriole for targeted destruction of HsSAs-6. Contrastingly, at normal conditions, however, FBXW7 showed an inverse localization pattern with respect to HsSAs-6. One explanation could be that most of the endogenous HsSAs-6 was degraded by the ligase before it could even accumulate to the mother centriole. The only exception is the procentriole assembly site, where HsSAs-6 recruitment is facilitated, but FBXW7 localization is minimal. However, determination of how FBXW7 localization is inhibited at the procentriole site requires future investigation. Overall, our data indicate that FBXW7 plays a major role in defining the site of procentriole assembly on the mother centriole.

HsSAs-6 protein level is controlled by degradation by APC/C-Cdh1 during late mitosis until G₁ (28) and by another F-box family ligase, SCF^{FBXW5}, during late S phase (32). However, APC/C-Cdh1 is inactivated as the cells progress to G₁/S due to degradation of its cyclin counterpart (45, 46). Similarly,

SCF^{FBXW5} activity is diminished sharply after G₂ due to FBXW5 degradation by APC/C-Cdc20 (32). Moreover, activity of Plk4 is high during G₁/S (33, 47, 48). The FBXW7 level is high at G₁ until G₁/S and starts to decrease as the cells proceed through S phase (40). We find here that HsSAs-6 degradation is maximal at G₁/S until early S phase (Fig. 3). This indicates that FBXW7-mediated centriole duplication control is primarily active during G₁/S until early S phase.

In conclusion, we have demonstrated that targeted degradation of HsSAs-6 by SCF^{FBXW7} is a key mechanism that controls centriole amplification.

Experimental procedures

Cell culture, gene silencing by siRNA

U2OS, HeLa, or HEK293T cells were originally obtained from ATCC. FBXW7 WT (FBXW7^{+/+}) and homozygous FBXW7^{-/-} knockout (KO) DLD-1 cell lines were obtained from the Vogelstein laboratory (Johns Hopkins University), and hTERT-RPE1-18 stable cells co-expressing CenpA-eGFP and centrin-1-eGFP were obtained from Alexey Khodjakov.

Co-IP

Cell lysates were incubated with antibodies as specified for immunoprecipitation, and proteins were pulled down.

Immunofluorescence microscopy

Methanol-fixed cells were incubated with primary antibodies followed by incubation with secondary antibodies. The images were captured by a Leica SP 5 laser confocal microscope.

SIM

The images were captured through a ×100 1.49 numerical aperture Apo Oil objective in an N-SIM microscope (Nikon).

Protein purification

Purification of MBP-HsSAs-6 was performed as described earlier (49).

Ubiquitination assays

In vivo ubiquitination assay—HsSAs-6 ubiquitination was assessed in G₁/S synchronized cells as described (50).

In vitro ubiquitination assay—Purified SCF^{FBXW7} complex (50) and Myc-HsSAs-6 protein (WT or 2A mutant) were mixed together, and ubiquitination was induced by E1, E2, and Ub protein.

Figure 5. SCF^{FBXW7} ubiquitylates HsSAs-6. *a*, HEK293T cells were transfected with HA-Ub and FLAG-FBXW7 or FLAG-FBXW7-WDΔ (24 h) followed by G₁/S synchronization by thymidine (18 h) and then MG-132 (6 h). Co-IPs of HsSAs-6 were probed for ubiquitylated proteins. *b*, recombinant MBP-tagged HsSAs-6 (1×, 2×, and 3×) bound with amylose resin was incubated separately with a mixture of SCF-FBXW7 components, Myc-Skp-1, Myc-Cul-1, HA-Rbx-1, and FLAG-FBXW7, followed by E1, E2, Ub, and ATP. Samples were immunoblotted for HsSAs-6 and ubiquitin. *c*, MBP-tagged HsSAs-6 mixed with either Ub WT or Ub K63R or Ub K48R mutants probed for ubiquitination as described in *b*. *d*, lysates of HEK293T cells transfected with FLAG-FBXW7 together with either Myc-HsSAs-6 WT or Myc-HsSAs-6 2A (S111A/T495A) were subjected to FLAG pulldown. *e*, Myc-HsSAs-6 protein (WT versus mutant) exogenously expressed and pulled down was mixed with SCF-FBXW7 and probed for ubiquitination (*top*). The same samples were probed for Myc-HsSAs-6 (*bottom*). *f*, confocal images of HeLa Kyoto cells transfected with HsSAs-6 3'-UTR siRNA followed by transfection with mCherry-HsSAs-6 WT or mCherry-HsSAs-6 2A and then G₁/S synchronized. Scale bar, 5 μm. The percentage of cells with centriole numbers in these conditions is plotted. *g*, HeLa Kyoto cells were transfected with HsSAs-6 3'-UTR siRNA followed by mCherry-HsSAs-6 WT or mCherry-HsSAs-6 2A, and the mitotic cells were imaged for CP110 and γ-tubulin. The plot shows percentage bipolar versus multipolar cells. *n* ≈ 70 cells in *f* and ~50 mitotic cells in *g*. In all of the plots, data are mean ± S.D. (error bars) (*n* = 3).

More details of the experimental procedures are provided in the supporting Experimental procedures.

Author contributions—B. B. and T. K. M. data curation; B. B., R. G., and T. K. M. formal analysis; B. B. validation; B. B., R. G., S. V. N., and A. C. investigation; B. B. visualization; B. B. methodology; B. B. and T. K. M. writing-review and editing; T. K. M. conceptualization; T. K. M. supervision; T. K. M. funding acquisition; T. K. M. writing-original draft; T. K. M. project administration.

Acknowledgments—We are grateful to Daiju Kitagawa, Pierre Gonczy, Bert Vogelstein, Alexey Khodjakov, Sachin Kotak, Wenyi Wei, and Bruce Clurman for plasmids and cell lines. We thank T. R. Santhoshkumar for support in SIM imaging.

References

- Levine, M. S., Bakker, B., Boeckx, B., Moyett, J., Lu, J., Vitre, B., Spierings, D. C., Lansdorp, P. M., Cleveland, D. W., Lambrechts, D., Foijer, F., and Holland, A. J. (2017) Centrosome amplification is sufficient to promote spontaneous tumorigenesis in mammals. *Dev. Cell* **40**, 313–322. [CrossRef Medline](#)
- Nigg, E. A., and Holland, A. J. (2018) Once and only once: mechanisms of centriole duplication and their deregulation in disease. *Nat. Rev. Mol. Cell Biol.* **19**, 297–312. [CrossRef Medline](#)
- Nigg, E. A., and Raff, J. W. (2009) Centrioles, centrosomes, and cilia in health and disease. *Cell* **139**, 663–678. [CrossRef Medline](#)
- Doxsey, S., Zimmerman, W., and Mikule, K. (2005) Centrosome control of the cell cycle. *Trends Cell Biol.* **15**, 303–311. [CrossRef Medline](#)
- Firat-Karalar, E. N., and Stearns, T. (2014) The centriole duplication cycle. *Philos. Trans. R. Soc. Lond. B Biol. Sci.* **369**, 20130460. [CrossRef Medline](#)
- Dammermann, A., Müller-Reichert, T., Pelletier, L., Habermann, B., Desai, A., and Oegema, K. (2004) Centriole assembly requires both centriolar and pericentriolar material proteins. *Dev. Cell* **7**, 815–829. [CrossRef Medline](#)
- Ganem, N. J., Godinho, S. A., and Pellman, D. (2009) A mechanism linking extra centrosomes to chromosomal instability. *Nature* **460**, 278–282. [CrossRef Medline](#)
- Gönczy, P., Echeverri, C., Oegema, K., Coulson, A., Jones, S. J., Copley, R. R., Duperon, J., Oegema, J., Brehm, M., Cassin, E., Hannak, E., Kirkham, M., Pichler, S., Flohrs, K., Goessen, A., et al. (2000) Functional genomic analysis of cell division in *C. elegans* using RNAi of genes on chromosome III. *Nature* **408**, 331–336. [CrossRef Medline](#)
- Gönczy, P. (2012) Towards a molecular architecture of centriole assembly. *Nat. Rev. Mol. Cell Biol.* **13**, 425–435. [CrossRef Medline](#)
- Sönnichsen, B., Koski, L. B., Walsh, A., Marschall, P., Neumann, B., Brehm, M., Alleaume, A. M., Artelt, J., Bettencourt-Dias, M., Cassin, E., Hewitson, M., Holz, C., Khan, M., Lazik, S., Martin, C., et al. (2005) Full-genome RNAi profiling of early embryogenesis in *Caenorhabditis elegans*. *Nature* **434**, 462–469. [CrossRef Medline](#)
- Brito, D. A., Gouveia, S. M., and Bettencourt-Dias, M. (2012) Deconstructing the centriole: structure and number control. *Curr. Opin. Cell Biol.* **24**, 4–13. [CrossRef Medline](#)
- Jana, S. C., Marteil, G., and Bettencourt-Dias, M. (2014) Mapping molecules to structure: unveiling secrets of centriole and cilia assembly with near-atomic resolution. *Curr. Opin. Cell Biol.* **26**, 96–106. [CrossRef Medline](#)
- Avidor-Reiss, T., and Gopalakrishnan, J. (2013) Building a centriole. *Curr. Opin. Cell Biol.* **25**, 72–77. [CrossRef Medline](#)
- Blachon, S., Gopalakrishnan, J., Omori, Y., Polyanovsky, A., Church, A., Nicastro, D., Malicki, J., and Avidor-Reiss, T. (2008) *Drosophila* asterless and vertebrate Cep152 are orthologs essential for centriole duplication. *Genetics* **180**, 2081–2094. [CrossRef Medline](#)
- Cizmeçioğlu, O., Arnold, M., Bahtz, R., Settele, F., Ehret, L., Haselmann-Weiss, U., Antony, C., and Hoffmann, I. (2010) Cep152 acts as a scaffold for recruitment of Plk4 and CPAP to the centrosome. *J. Cell Biol.* **191**, 731–739. [CrossRef Medline](#)
- Dzhindzhev, N. S., Yu, Q. D., Weiskopf, K., Tzolovsky, G., Cunha-Ferreira, I., Riparbelli, M., Rodrigues-Martins, A., Bettencourt-Dias, M., Callaini, G., and Glover, D. M. (2010) Asterless is a scaffold for the onset of centriole assembly. *Nature* **467**, 714–718. [CrossRef Medline](#)
- Hatch, E. M., Kulukian, A., Holland, A. J., Cleveland, D. W., and Stearns, T. (2010) Cep152 interacts with Plk4 and is required for centriole duplication. *J. Cell Biol.* **191**, 721–729. [CrossRef Medline](#)
- Kitagawa, D., Vakonakis, I., Olieric, N., Hilbert, M., Keller, D., Olieric, V., Bortfeld, M., Erat, M. C., Flückiger, I., Gönczy, P., and Steinmetz, M. O. (2011) Structural basis of the 9-fold symmetry of centrioles. *Cell* **144**, 364–375. [CrossRef Medline](#)
- Guichard, P., Hachet, V., Majubu, N., Neves, A., Demurtas, D., Olieric, N., Flückiger, I., Yamada, A., Kihara, K., Nishida, Y., Moriya, S., Steinmetz, M. O., Hongoh, Y., and Gönczy, P. (2013) Native architecture of the centriole proximal region reveals features underlying its 9-fold radial symmetry. *Curr. Biol.* **23**, 1620–1628. [CrossRef Medline](#)
- Hilbert, M., Noga, A., Frey, D., Hamel, V., Guichard, P., Kraatz, S. H., Pfreundschuh, M., Hosner, S., Flückiger, I., Jaussi, R., Wieser, M. M., Thielges, K. M., Deupi, X., Müller, D. J., Kammerer, R. A., et al. (2016) SAS-6 engineering reveals interdependence between cartwheel and microtubules in determining centriole architecture. *Nat. Cell Biol.* **18**, 393–403. [CrossRef Medline](#)
- Guichard, P., Hamel, V., Le Guennec, M., Banterle, N., Iacovache, I., Nemčíková, V., Flückiger, I., Goldie, K. N., Stahlberg, H., Lévy, D., Zuber, B., and Gönczy, P. (2017) Cell-free reconstitution reveals centriole cartwheel assembly mechanisms. *Nat. Commun.* **8**, 14813. [CrossRef Medline](#)
- Nakazawa, Y., Hiraki, M., Kamiya, R., and Hirono, M. (2007) SAS-6 is a cartwheel protein that establishes the 9-fold symmetry of the centriole. *Curr. Biol.* **17**, 2169–2174. [CrossRef Medline](#)
- van Breugel, M., Hirono, M., Andreeva, A., Yanagisawa, H. A., Yamaguchi, S., Nakazawa, Y., Morgner, N., Petrovich, M., Ebong, I. O., Robinson, C. V., Johnson, C. M., Veprintsev, D., and Zuber, B. (2011) Structures of SAS-6 suggest its organization in centrioles. *Science* **331**, 1196–1199. [CrossRef Medline](#)
- van Breugel, M., Wilcken, R., McLaughlin, S. H., Rutherford, T. J., and Johnson, C. M. (2014) Structure of the SAS-6 cartwheel hub from *Leishmania major*. *eLife* **3**, e01812. [CrossRef Medline](#)
- Leidel, S., Delattre, M., Cerutti, L., Baumer, K., and Gönczy, P. (2005) SAS-6 defines a protein family required for centrosome duplication in *C. elegans* and in human cells. *Nat. Cell Biol.* **7**, 115–125. [CrossRef Medline](#)
- Hilbert, M., Erat, M. C., Hachet, V., Guichard, P., Blank, I. D., Flückiger, I., Slater, L., Lowe, E. D., Hatzopoulos, G. N., Steinmetz, M. O., Gönczy, P., and Vakonakis, I. (2013) *Caenorhabditis elegans* centriolar protein SAS-6 forms a spiral that is consistent with imparting a ninefold symmetry. *Proc. Natl. Acad. Sci. U.S.A.* **110**, 11373–11378. [CrossRef Medline](#)
- Gupta, H., Badarudeen, B., George, A., Thomas, G. E., Gireesh, K. K., and Manna, T. K. (2015) Human SAS-6 C-terminus nucleates and promotes microtubule assembly *in vitro* by binding to microtubules. *Biochemistry* **54**, 6413–6422. [CrossRef Medline](#)
- Strnad, P., Leidel, S., Vinogradova, T., Euteneuer, U., Khodjakov, A., and Gönczy, P. (2007) Regulated HsSAS-6 levels ensure formation of a single procentriole per centriole during the centrosome duplication cycle. *Dev. Cell* **13**, 203–213. [CrossRef Medline](#)
- Kleylein-Sohn, J., Westendorf, J., Le Clech, M., Habedanck, R., Stierhof, Y. D., and Nigg, E. A. (2007) Plk4-induced centriole biogenesis in human cells. *Dev. Cell* **13**, 190–202. [CrossRef Medline](#)
- Sonnen, K. F., Schermelleh, L., Leonhardt, H., and Nigg, E. A. (2012) 3D-structured illumination microscopy provides novel insight into architecture of human centrosomes. *Biol. Open* **1**, 965–976. [CrossRef Medline](#)
- Peel, N., Stevens, N. R., Basto, R., and Raff, J. W. (2007) Overexpressing centriole-replication proteins *in vivo* induces centriole overduplication and *de novo* formation. *Curr. Biol.* **17**, 834–843. [CrossRef Medline](#)
- Puklowski, A., Homsy, Y., Keller, D., May, M., Chauhan, S., Kossatz, U., Grünwald, V., Kubicka, S., Pich, A., Manns, M. P., Hoffmann, I., Gönczy, P., and Malek, N. P. (2011) The SCF-FBXW5 E3-ubiquitin ligase is regulated by PLK4 and targets HsSAS-6 to control centrosome duplication. *Nat. Cell Biol.* **13**, 1004–1009. [CrossRef Medline](#)

33. Guderian, G., Westendorf, J., Uldschmid, A., and Nigg, E. A. (2010) Plk4 trans-autophosphorylation regulates centriole number by controlling betaTrCP-mediated degradation. *J. Cell Sci.* **123**, 2163–2169 [CrossRef Medline](#)
34. Arquint, C., and Nigg, E. A. (2014) STIL microcephaly mutations interfere with APC/C-mediated degradation and cause centriole amplification. *Curr. Biol.* **24**, 351–360 [CrossRef Medline](#)
35. D'Angiolella, V., Donato, V., Vijayakumar, S., Saraf, A., Florens, L., Washburn, M. P., Dynlacht, B., and Pagano, M. (2010) SCF(Cyclin F) controls centrosome homeostasis and mitotic fidelity through CPl10 degradation. *Nature* **466**, 138–142 [CrossRef Medline](#)
36. Davis, R. J., Welcker, M., and Clurman, B. E. (2014) Tumor suppression by the Fbw7 ubiquitin ligase: mechanisms and opportunities. *Cancer Cell* **26**, 455–464 [CrossRef Medline](#)
37. Akhondji, S., Sun, D., von der Lehr, N., Apostolidou, S., Klotz, K., Maljukova, A., Cepeda, D., Fiegl, H., Dofou, D., Marth, C., Mueller-Holzner, E., Corcoran, M., Dagnell, M., Nejad, S. Z., Nayer, B. N., *et al.* (2007) FBXW7/hCDC4 is a general tumor suppressor in human cancer. *Cancer Res.* **67**, 9006–9012 [CrossRef Medline](#)
38. Rajagopalan, H., Jallepalli, P. V., Rago, C., Velculescu, V. E., Kinzler, K. W., Vogelstein, B., and Lengauer, C. (2004) Inactivation of hCDC4 can cause chromosomal instability. *Nature* **428**, 77–81 [CrossRef Medline](#)
39. Maskey, D., Marlin, M. C., Kim, S., Kim, S., Ong, E. C., Li, G., and Tsiokas, L. (2015) Cell cycle-dependent ubiquitylation and destruction of NDE1 by CDK5-FBW7 regulates ciliary length. *EMBO J.* **34**, 2424–2440 [CrossRef Medline](#)
40. Cizmecioglu, O., Krause, A., Bahtz, R., Ehret, L., Malek, N., and Hoffmann, I. (2012) Plk2 regulates centriole duplication through phosphorylation-mediated degradation of Fbxw7 (human Cdc4). *J. Cell Sci.* **125**, 981–992 [CrossRef Medline](#)
41. Zou, C., Li, J., Bai, Y., Gunning, W. T., Wazer, D. E., Band, V., and Gao, Q. (2005) Centrobin: a novel daughter centriole-associated protein that is required for centriole duplication. *J. Cell Biol.* **171**, 437–445 [CrossRef Medline](#)
42. Skaar, J. R., Pagan, J. K., and Pagano, M. (2013) Mechanisms and function of substrate recruitment by F-box proteins. *Nat. Rev. Mol. Cell Biol.* **14**, 369–381 [CrossRef Medline](#)
43. Ohtake, F., Saeki, Y., Ishido, S., Kanno, J., and Tanaka, K. (2016) The K48-K63 branched ubiquitin chain regulates NF- κ B signaling. *Mol. Cell* **64**, 251–266 [CrossRef Medline](#)
44. Mao, J. H., Kim, I. J., Wu, D., Climent, J., Kang, H. C., DelRosario, R., and Balmain, A. (2008) FBXW7 targets mTOR for degradation and cooperates with PTEN in tumor suppression. *Science* **321**, 1499–1502 [CrossRef Medline](#)
45. García-Higuera, I., Manchado, E., Dubus, P., Cañamero, M., Méndez, J., Moreno, S., and Malumbres, M. (2008) Genomic stability and tumour suppression by the APC/C cofactor Cdh1. *Nat. Cell Biol.* **10**, 802–811 [CrossRef Medline](#)
46. Skaar, J. R., and Pagano, M. (2008) Cdh1: a master G₀/G₁ regulator. *Nat. Cell Biol.* **10**, 755–757 [CrossRef Medline](#)
47. Holland, A. J., Lan, W., Niessen, S., Hoover, H., and Cleveland, D. W. (2010) Polo-like kinase 4 kinase activity limits centrosome overduplication by autoregulating its own stability. *J. Cell Biol.* **188**, 191–198 [CrossRef Medline](#)
48. Sillibourne, J. E., Tack, F., Vloemans, N., Boeckx, A., Thambirajah, S., Bonnet, P., Ramaekers, F. C., Bornens, M., and Grand-Perret, T. (2010) Autophosphorylation of polo-like kinase 4 and its role in centriole duplication. *Mol. Biol. Cell* **21**, 547–561 [CrossRef Medline](#)
49. Ohta, M., Ashikawa, T., Nozaki, Y., Kozuka-Hata, H., Goto, H., Inagaki, M., Oyama, M., and Kitagawa, D. (2014) Direct interaction of Plk4 with STIL ensures formation of a single procentriole per parental centriole. *Nat. Commun.* **5**, 5267 [CrossRef Medline](#)
50. Inuzuka, H., Shaik, S., Onoyama, I., Gao, D., Tseng, A., Maser, R. S., Zhai, B., Wan, L., Gutierrez, A., Lau, A. W., Xiao, Y., Christie, A. L., Aster, J., Settleman, J., Gygi, S. P., Kung, A. L., Look, T., Nakayama, K. I., DePino, R. A., and Wei, W. (2011) SCF(FBW7) regulates cellular apoptosis by targeting MCL1 for ubiquitylation and destruction. *Nature* **471**, 104–109 [CrossRef Medline](#)